[2]Masad, J. A., and Malik, M. R., "On the Link Between Flow Separation and Transition Onset," AIAA Paper 94-2370, 1994.
[3]Davis, R. T., "A Procedure for Solving the Compressible Interacting Boundary Layer Equations for Subsonic and Supersonic Flows," AIAA Paper 84-1614, 1984.
[4]Abu Khajeel, H. T., "Effect of Humps on the Stability of Boundary Layers over an Airfoil," M.S. Thesis, Virginia Polytechnic Inst. and State Univ., Blacksburg, VA, 1993.
[5]Mack, L. M., "Boundary-Layer Stability Theory," Jet Propulsion Lab., Document 900-277 (Rev. A), Pasadena, CA, 1969.
[6]Pereyra, V., "PASVA3: An Adaptive Finite-Difference Fortran Program for First-Order Nonlinear Ordinary Boundary-Value Problems," *Lecture Notes on Computer Science*, Vol. 76, 1976, p. 67.
[7]Smith, A. M. O., and Gamberoni, N., "Transition Pressure Gradient, and Stability Pressure Theory," Douglas Aircraft Co., Rept. ES 25388, El Segundo, CA, 1956.
[8]Jaffe, N. A., Okamura, T. T., and Smith, A. M. O., "Determination of Spatial Amplification Factors and Their Application to Predicting Transition," *AIAA Journal*, Vol. 8, No. 2, 1970, pp. 301–308.
[9]Masad, J. A., and Nayfeh, A. H., "Laminar Flow Control of Subsonic Boundary Layers by Suction and Heat-Transfer Strips," *Physics of Fluids A*, Vol. 4, No. 6, 1992, pp. 1259–1272.
[10]Reynolds, G. A., and Saric, W. S., "Experiments on the Stability of Flat-Plate Boundary Layer with Suction," *AIAA Journal*, Vol. 24, No. 2, 1986, pp. 202–207.
[11]Saric, W. S., and Reed, H. L., "Effect of Suction and Weak Mass Injection on Boundary-Layer Transition," *AIAA Journal*, Vol. 24, No. 3, 1986, pp. 383–389.

Actuator Placement with Failure Consideration for Static Shape Control of Truss Structures

Saburo Matunaga*
Tokyo Institute of Technology, Tokyo 152, Japan
and
Junjiro Onoda†
Institute of Space and Astronautical Science, Sagamihara 229, Japan

Introduction

ACTIVE control using actuators to obtain high accuracy of the static shape of large space structures is proposed. Unlike vibration control, high-control performance in static shape control is primarily determined by actuator location. A great deal of effort has been made in the last few years on techniques for solving for the optimal actuator placement or the integer optimization problem.[1,2] What seems to be lacking, however, is to evaluate the fault tolerance of the obtained actuator placement. In this Note, actuator failures are taken into consideration in the process of optimization.[3] In space applications actuator failure may occur, for example, at liftoff of the rocket, in the process of deployment and construction of the space structures and during operation of the actuators. Because it is so costly to repair or exchange a failed actuator in space, the actuators should be located so as to meet mission requirements even in the event of failure.

In this Note, actuator failure models are classified and their formulation is given. The optimization problem in this study is explained, and the results of computational simulations using a realistic example are discussed. The genetic algorithm (GA) method is used as the optimizer in these simulations.

Received Aug. 18, 1994; revision received Jan. 19, 1995; accepted for publication Jan. 20, 1995.

*Research Associate, Department of Mechano-Aerospace Engineering, Meguro-ku. Member AIAA.
†Professor, Research Division of Space Transportation, Yoshinodai. Member AIAA.

Optimal Shape Control Law

It is assumed that static distortion has occurred due to errors in the element length of truss structures e. When the system is assumed to be linear, the sensed distortion $\boldsymbol{u}$ is obtained as[4]

$$\boldsymbol{u} = \Psi \boldsymbol{e} + \boldsymbol{B}\theta = \psi + \boldsymbol{B}\theta \tag{1}$$

where ψ is the distortion caused by the length errors of the truss members, $\boldsymbol{\theta}$ is the vector of actuations of the actuators, and Ψ and $\boldsymbol{B}$ are the matrices which represent their effects. The quadratic distortion measure can be expressed by a proper weighting matrix $\boldsymbol{W}$ as follows:

$$u_{\text{rms}}^2 = \boldsymbol{u}^T \boldsymbol{W} \boldsymbol{u} \tag{2}$$

The actuators are controlled such that the quadratic measure is minimized based on the measured distortion, then the residual distortion and distortion measure after the optimal control become

$$\delta \equiv \boldsymbol{u}_{\text{opt}} = (\boldsymbol{I} - \boldsymbol{B}\boldsymbol{A}^{-1}\boldsymbol{B}^T\boldsymbol{W})\psi = \boldsymbol{G}\psi \tag{3}$$

$$\delta_{\text{rms}}^2 = \psi^T(\boldsymbol{W} - \boldsymbol{W}\boldsymbol{B}\boldsymbol{A}^{-1}\boldsymbol{B}^T\boldsymbol{W})\psi = \psi^T\boldsymbol{Q}\psi \tag{4}$$

where $\boldsymbol{A} = \boldsymbol{B}^T\boldsymbol{W}\boldsymbol{B}$. The effectiveness of the shape correction is measured by, e.g.,[4]

$$g^2 = E\left[\delta_{\text{rms}}^2\right]/E[\psi^T\boldsymbol{W}\psi] = \text{tr}[\boldsymbol{Q}\boldsymbol{C}_{\psi\psi}]/\text{tr}[\boldsymbol{W}\boldsymbol{C}_{\psi\psi}] \tag{5}$$

where $E[\,]$ denotes the expectation, tr[ ] refers to the trace of matrix[ ], and $\boldsymbol{C}_{\psi\psi}$ is the covariance matrix obtained from the covariance matrix of e.

Actuator Failure Models

Classification

Actuator failure models are considered in this section.[3] They may be divided into two main types as control system can identify the failed actuator A-1, and control system can not identify the failed actuator A-2. They can be further classified into the following three types, when an actuator is failed, the failed actuator fastens the member B-1, the failed actuator releases the member B-2, and the failed actuator actuator out of control B-3. Moreover, B-1 may be grouped into the following: the length of the failed active member is fixed to the initial length, in other words, it is regarded as a passive member B-1-1, and the length is fixed to the last length under control B-1-2, namely, it is regarded as the passive member whose length error is superimposed with the last actuated value of the actuator, where it is understood that the control effectiveness is not affected by the actuator's stiffness provided its stroke is long enough.[2] We can divide B-3 into two types: the actuated value of the failed actuator is correlated with the control value B-3-1, and the actuated value is not correlated with the control value B-3-2.

Formulation

In this Note, we concentrate on the simplest failure model: A-1 and B-1-1. The number of failed actuators is assumed to be only one, though it is easy to extend the analysis to several failed actuators. Similar to Haftka and Adelman,[1] this section develops a rigorous evaluation of the control measure, Eq. (5), due to removing one actuator. Removing the ith actuator can be simulated by performing the minimization of Eq. (2) under the constraint that $\theta_i = 0$. Employing Lagrange multipliers, we search for stationary points of ϕ_i where

$$\phi_i = \boldsymbol{u}^T\boldsymbol{W}\boldsymbol{u} - 2\lambda \boldsymbol{e}_{fi}^T\theta \tag{6}$$

where $\boldsymbol{e}_{fi}$ is a vector with unity in the ith row and zeros elsewhere, and $\boldsymbol{e}_{fi}^T\theta = \theta_i$. From stationary conditions, the distortion measure, Eq. (2), becomes

$$\delta_{\text{rms}}^{2(i)} = \psi^T\boldsymbol{Q}\psi + \lambda \boldsymbol{e}_{fi}^T\boldsymbol{S}\psi + \lambda^2 \boldsymbol{e}_{fi}^T\boldsymbol{U}\boldsymbol{e}_{fi} \tag{7}$$

where $\boldsymbol{H} = \boldsymbol{I} - \boldsymbol{G}$, $\boldsymbol{S} = \boldsymbol{HG} + (\boldsymbol{HG})^T$, and $\boldsymbol{U} = \boldsymbol{HBA}^{-1}$. Then using Eq. (4),

$$E\left[\delta_{\text{rms}}^{2(i)}\right] = E\left[\delta_{\text{rms}}^2\right] + \Delta^{(i)} E\left[\delta_{\text{rms}}^2\right] \tag{8}$$

where

$$\Delta^{(i)} E\left[\delta_{\text{rms}}^2\right] = 1/a^{-1}{}_{ii} \Sigma_{j \le k} (H_{ij} S_{ik} + S_{ij} H_{ik}) C_{\psi\psi,jk} + 2U_{ii} / \left(a^{-1}{}_{ii}\right)^2 \Sigma_{j \le k} H_{ij} H_{ik} C_{\psi\psi,jk} \tag{9}$$

$a^{-1}{}_{ii}$ is the ith diagonal of A^{-1}, and H_{ij}, S_{ij}, U_{ij}, and $C_{\psi\psi,ij}$ are ij components of $\boldsymbol{H}$, $\boldsymbol{S}$, $\boldsymbol{U}$, and $C_{\psi\psi}$, respectively.

Therefore, we can obtain the following equations from Eq. (5):

$$g^{2(i)} = g^2 + \Delta^{(i)} g^2 \tag{10}$$

$$\Delta^{(i)} g^2 = \Delta^{(i)} E\left[\delta_{\text{rms}}^2\right] / E[\psi^T \boldsymbol{W} \psi] \tag{11}$$

Optimization Problem and Numerical Example

The optimal problem of the present Note is the following min-max problem:

$$\text{Minimize}_{I=\{x_1,x_2,\ldots,x_{n_a}\}} \bar{g}^2(I) = g^2 + \max_{1 \le i \le n_a} \Delta^{(i)} g^2$$

subject to

$$x_j \in \{1, 2, \ldots, n_e\} \qquad (j = 1, 2, \ldots, n_a)$$

Hence, we look for the actuator placement in which the worst value of the control measure due to one failed actuator is a minimum.

This problem is demonstrated by using a three-ring tetrahedral parabolic truss[2] as shown in Fig. 1. This structure is composed of a total of 234 members, that is, 90 upper-surface members, 63 lower-surface members, and 81 core members. The number of actuators n_a is limited to 10. We assume that only one actuator among 10 fails. As a result, the total number of feasible configurations amounts to 4.1×10^{23} for case A in which more than one actuator can be accepted in a single member, and 1.1×10^{17} for case B in which only one actuator is accepted. As such, we obtain not the exact best solution but the approximately optimal one.

The component of the ith row and the jth column of the covariance matrix of the length error is given as[2] $\Sigma_{ij} = 1.0 \times 10^{-4}(\delta_{ij} + \gamma_{ij})$, where δ_{ij} is the Kronecker delta, and $\gamma_{ij} = 1$ if both i and j are on the lower or upper surface, $\gamma_{ij} = 0$ if i or j are in a core member, $\gamma_{ij} = -1$ otherwise. The displacements in the z direction of 37 nodes on the upper surface are sensed. In this study, the GA method is used as the optimizer in which population number is 50, the probability of mutation is 0.05, and the total number of selected configurations in one calculation is 60,000 (Ref. 2).

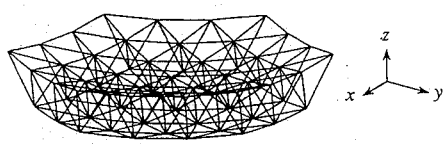

Fig. 1 Parabolic three-ring tetrahedral truss structure.

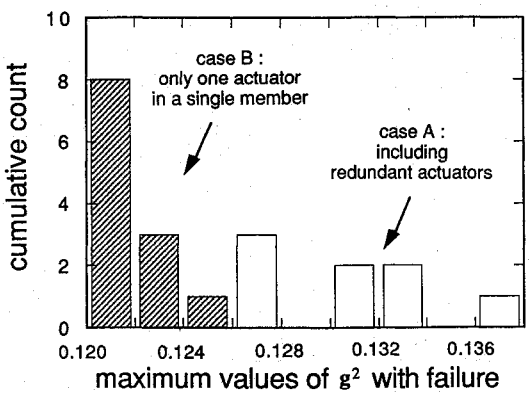

Fig. 2 Histogram of the worst value of g^2 with one actuator failure.

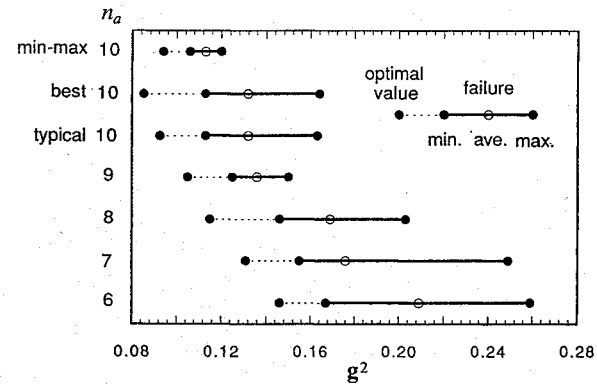

Fig. 3 Comparison of the value of g^2.

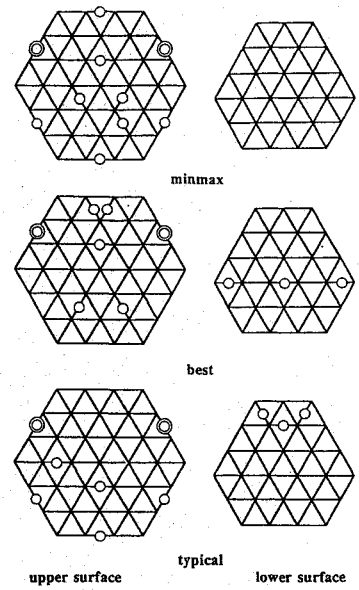

Fig. 4 Configurations of the optimal actuator placement.

Figure 2 shows a histogram of the results of a total of 20 calculations, in other words, 8 for case A and 12 for case B, and indicates that case B is superior to case A. The best placement ($g^2 = 0.094$, $\max g^{2(i)} = 0.120$) of the min-max problem was obtained five times in 12 calculations.

Figure 3 summarizes the comparison of the control measures of the optimal placement for the min-max problem and of the optimal ones without failure consideration in various actuator numbers, n_a. In Fig. 3, min-max is the optimal value of the control measure with failure consideration, best and typical denote the best optimal value and the optimal value obtained many times without failure consideration, respectively, min., ave., and max. designate the minimum, average, and maximum values in the case that 1 actuator in n_a actuators has failed. Figure 3 indicates that the optimal value of min-max is better than the optimal value of $n_a = 9$, and that the maximum value of min-max in the case of failure is superior to the optimal value of $n_a = 7$. The average value is nearly equal to the optimal value of $n_a = 8$, and the minimum value is not very much inferior to the optimal value of $n_a = 9$. In the best and typical cases, however, the values of the control measure become by far worse when 1 actuator has failed.

The configurations of the optimal actuator placement obtained in this study are shown in Fig. 4. The circle denotes the active member, and the double circle designates the critical member among the active members if an actuator failure has occurred. Figure 4 tells us that it is difficult to obtain good actuator location against an actuator failure without failure consideration.

Concluding Remarks

The authors propose an actuator location optimization with actuator failure consideration for the static shape control of truss structures. Actuator failure models are considered, and the formulation of

the simplest failure model is given. The authors explain that the optimization problem of the present study becomes a min-max problem. This analysis is applied to a realistic problem based on a three-ring tetrahedral truss example. So far as investigated here, an actuator location with high fault tolerance for static shape control can be obtained by an optimization with actuator failure consideration.

Acknowledgments

Our special thanks are due to Prof. Ohkami of the Tokyo Institute of Technology for his valuable advice and to Mr. Hanawa of the University of Tokyo for helpful discussions.

References

[1]Haftka, R. T., and Adelman, H. M., "Selection of Actuator Locations for Static Shape Control of Large Space Structures by Heuristic Integer Programming," *Computers and Structures*, Vol. 20, No. 1–3, 1985, pp. 575–582.

[2]Onoda, J., and Hanawa, Y., "Actuator Placement Optimization by Genetic and Improved Simulated Annealing Algorithms," *AIAA Journal*, Vol. 31, No. 6, 1993, pp. 1167–1169.

[3]Matunaga, S., and Onoda, J., "Actuator Location Optimization for Static Shape Control with Actuator Failure Consideration," *Proceedings 8th Space Structures Symposium* (Kanagawa, Japan), 1992, pp. 76–81.

[4]Burdisso, R. A., and Haftka, R. T., "Statistical Analysis of Static Shape Control in Space Structures," *AIAA Journal*, Vol. 28, No. 8, 1990, pp. 1504–1508.

Zigzag Theory for Composite Laminates

Xiaoyu Li* and Dahsin Liu†
Michigan State University,
East Lansing, Michigan 48824

Fundamentals

HIGH-ORDER shear deformation theories (HSDT) have been widely used in composite laminate analysis. Lo et al.[1] have used unified notations to document the development of HSDT according to the order of thickness coordinate z of the assumed in-plane displacements. As a result, they have also presented a third-order shear deformation theory for composite laminate analysis, i.e.,

$$\begin{aligned} u(x,y,z) &= u_0(x,y) + u_1(x,y)z + u_2(x,y)z^2 + u_3(x,y)z^3 \\ v(x,y,z) &= v_0(x,y) + v_1(x,y)z + v_2(x,y)z^2 + v_3(x,y)z^3 \\ w(x,y,z) &= w_0(x,y) + w_1(x,y)z + w_2(x,y)z^2 \end{aligned} \tag{1}$$

The predictions of in-plane stresses from HSDT are reasonably good. However, with the assumptions of continuous functions of u and v through the laminate thickness, the kinky, zigzag distribution of in-plane displacements cannot be obtained from HSDT. To remove the deficiency and to improve the accuracy of transverse stress prediction, layerwise theories (LT), which are based on assumed displacements for individual layers, have been proved to be very promising techniques. A third-order layerwise theory has been presented by Lu and Liu[2] and can be expressed by the unified notations as used in Eqs. (1),

$$\begin{aligned} u^k(x,y,z) &= u_0^k(x,y) + u_1^k(x,y)z + u_2^k(x,y)z^2 + u_3^k(x,y)z^3 \\ v^k(x,y,z) &= v_0^k(x,y) + v_1^k(x,y)z + v_2^k(x,y)z^2 + v_3^k(x,y)z^3 \\ w(x,y,z) &= w_0(x,y) + w_1(x,y)z + w_2(x,y)z^2 \end{aligned} \tag{2}$$

where the superscript k represents the layer order.

Although the layerwise theory gives excellent displacements and stresses (both in-plane and transverse), it suffers from a major computational drawback. The total number of degrees of freedom is dependent on the number of composite layers. As the layer number increases, the computational effort becomes very demanding. As for compromising techniques to HSDT and LT, a few zigzag theories (ZT) based on different displacement fields have been developed, e.g., Refs. 3–7. This study aims at presenting a zigzag theory by utilizing the same notations as those used in Eqs. (2).

By following Eqs. (2), the in-plane displacements for each composite layer are assumed to consist of up to third-order terms. To have the total number of degrees of freedom independent of layer number, only two coefficients of u_i are allowed to be layer dependent. The remaining two coefficients are layer-independent variables. Since the characteristic of the zigzag theories is that only their zeroth-order and first-order terms are designated as layer dependent, the displacements of the kth layer of a zigzag theory can be defined as follows:

$$\begin{aligned} u^k(x,y,z) &= u_0^k(x,y) + u_1^k(x,y)z + u_2(x,y)z^2 + u_3(x,y)z^3 \\ w^k(x,y,z) &= w_0(x,y) + w_1(x,y)z + w_2(x,y)z^2 \end{aligned} \tag{3}$$

It should be noted that Eqs. (3) are for a two-dimensional, third-order theory. A more generalized theory that contains high-order terms can certainly be established. In addition, it is worthwhile to point out that the coefficients of the in-plane displacement polynomial are variables to be determined by variational process and continuity conditions on the laminate interfaces instead of special functions as defined in other zigzag theories. Details of the coordinates, layer order, and interface locations can be found in Fig. 1.

In this study, linear strain-displacement relations are employed:

$$\varepsilon_x^k = \frac{\partial u^k}{\partial x} \qquad \varepsilon_z^k = \frac{\partial w^k}{\partial z} \qquad \gamma_{xz}^k = \frac{\partial u^k}{\partial z} + \frac{\partial w^k}{\partial x} \tag{4}$$

Since the primary objective of this study is to evaluate the proposed zigzag theory, a closed-form solution that is free from numerical error is highly desired. As a consequence, only cross-ply laminates are considered. (For other composite laminations, numerical analysis such as finite element method is required.) The constitutive equations for the kth layer are given by

$$\begin{Bmatrix} \sigma_x^k \\ \sigma_z^k \\ \tau_{xy}^k \end{Bmatrix} = \begin{bmatrix} Q_{11}^k & Q_{13}^k & 0 \\ Q_{13}^k & Q_{33}^k & 0 \\ 0 & 0 & Q_{55}^k \end{bmatrix} \begin{bmatrix} \varepsilon_x^k \\ \varepsilon_z^k \\ \gamma_{xz}^k \end{bmatrix} \tag{5}$$

where Q_{ij}^k are stiffness components.

Formulation

Based on Eqs. (3), the number of layer-dependent variables in an n-layer composite laminate is $2n$. These variables can be replaced by layer-independent variables through the enforcement of continuity conditions of both displacement and transverse shear stress on the laminate interfaces. If the composite laminate has perfect bonding on the interfaces, the following continuity conditions should be satisfied:

$$\begin{aligned} u^{k-1}\big|_{z=z_k} &= u^k\big|_{z=z_k} \\ \tau_{xz}^{k-1}\big|_{z=z_k} &= \tau_{xz}^k\big|_{z=z_k} \end{aligned} \qquad k = 2, 3, 4, \ldots, n \tag{6}$$

By substituting Eqs. (3–5) into Eqs. (6), u_0^k and u_1^k are no longer layer-dependent variables. They can be replaced by two new layer-independent variables u_0 and u_1. And the coefficients of the polynomial equation are functions of layer properties and coordinates, i.e.,

$$\begin{aligned} u^k &= u_0 + \left(R_1^k + A_1^k z\right)u_1 + \left(R_2^k + A_2^k z + z^2\right)u_2 \\ &\quad + \left(R_3^k + A_3^k z + z^3\right)u_3 + \left(R_4^k + A_4^k z\right)w_{0,x} \\ &\quad + \left(R_5^k + A_5^k z\right)w_{1,x} + \left(R_6^k + A_6^k z\right)w_{2,x} \\ w^k(x,y,z) &= w_0(x,y) + w_1(x,y)z + w_2(x,y)z^2 \end{aligned} \tag{7}$$

Received Jan. 21, 1994; revision received Aug. 30, 1994; accepted for publication Sept. 2, 1994.

*Graduate Research Assistant, Department of Materials Science and Mechanics. Member AIAA.

†Associate Professor, Department of Materials Science and Mechanics. Member AIAA.